Fat Signal Suppression for Coronary MRA at 3T Using a Water-Selective Adiabatic T_2-Preparation Technique

Andrew J. Coristine,[1,2] Ruud B. van Heeswijk,[1,2] and Matthias Stuber[1,2]*

Purpose: To improve fat saturation in coronary MRA at 3T by using a spectrally selective adiabatic T_2-Prep (WSA-T_2-Prep).
Methods: A conventional adiabatic T_2-Prep (CA-T_2-Prep) was modified, such that the excitation and restoration pulses were of differing bandwidths. On-resonance spins are T_2-Prepared, whereas off-resonance spins, such as fat, are spoiled. This approach was combined with a CHEmically Selective Saturation (CHESS) pulse to achieve even greater fat suppression. Numerical simulations were followed by phantom validation and in vivo coronary MRA.
Results: Numerical simulations demonstrated that augmenting a CHESS pulse with a WSA-T_2-Prep improved robustness to B_1 inhomogeneities and that this combined fat suppression was effective over a broader spectral range than that of a CHESS pulse in a conventional T_2-Prepared sequence. Phantom studies also demonstrated that the WSA-T_2-Prep+CHESS combination produced greater fat suppression across a range of B_1 values than did a CA-T_2-Prep+CHESS combination. Lastly, in vivo measurements demonstrated that the contrast-to-noise ratio between blood and myocardium was not adversely affected by using a WSA-T_2-Prep, despite the improved abdominal and epicardial fat suppression. Additionally, vessel sharpness improved.
Conclusion: The proposed WSA-T_2-Prep method was shown to improve fat suppression and vessel sharpness as compared to a CA-T_2-Prep technique, and to also increase fat suppression when combined with a CHESS pulse. **Magn Reson Med 72:763–769, 2014. © 2013 Wiley Periodicals, Inc.**

Key words: adiabatic; coronary; fat; saturation; suppression; T_2-Prep

INTRODUCTION

In MRI of the heart, it is often desirable to suppress fat signal, as evidenced by the numerous fat saturation strategies available (inversion recovery, dual inversion, saturation bands, spectrally selective pulses, adiabatic frequency-selection, Dixon-based approaches, etc...) (1–5). Epicardial fat signal may decrease contrast between the coronary lumen and surrounding tissue and can lead to artificial vessel "narrowing" by means of water-fat signal cancellation. Meanwhile, abdominal fat signal may accentuate motion artifacts or decrease image quality through the introduction of unwanted background signal. In either case, these effects are more pronounced at higher field strengths, where inhomogeneities in the main magnetic field, B_0, and in the radiofrequency excitation field, B_1, complicate conventional fat saturation strategies (4,6), such as CHEmically Selective Saturation (CHESS) pulses (3), which are dependent on precise excitation angles and precessional frequencies.

Meanwhile, cardiac MRI frequently makes use of magnetization preparation modules, such as T_2 preparation (or T_2-Prep) (7), which is used to improve the contrast between blood and myocardium (8) in coronary MRA (9) and in myocardial T_2 mapping (10). At 1.5 Tesla (T), T_2-Prep methods generally use a nonselective $+90^\circ$, 180°, 180°, -90° pulse train (7) (or variant thereof), whereas at 3T, the 180° pulses may be made adiabatic (11) to address field inhomogeneities and to ensure a more uniform T_2 weighting.

In this study, we propose a simple bandwidth modification of the adiabatic T_2-Prep to combine T_2-weighting with an intrinsic fat signal suppression. This approach, dubbed the "Water-Selective Adiabatic T_2-Prep" (WSA-T_2-Prep) may be used alone or in combination with a conventional CHESS pulse. Numerical simulations of fat suppression efficacy versus B_0 and B_1 were performed to compare the robustness of the WSA-T_2-Prep+CHESS combination to that of a conventional adiabatic T_2-Prep (CA-T_2-Prep)+CHESS pulse. Phantom studies were then performed to validate these results, where the residual fat signal was measured across a range of CHESS pulse radiofrequency (RF) excitation angles. Finally, in vivo scans of the right coronary artery (RCA) were performed in healthy volunteers, and the fat suppression efficacy of each approach was measured in both the epicardium and abdomen. Signal to noise ratio (SNR) and contrast to noise ratio (CNR) were also measured for select tissues, along with vessel sharpness of the RCA.

METHODS

Background

A conventional electrocardiograph (ECG)-triggered coronary MRA sequence consists of a navigator for

[1]Department of Radiology, University Hospital (CHUV) / University of Lausanne (UNIL), Lausanne, VD, Switzerland.
[2]CardioVascular Magnetic Resonance (CVMR), Research Centre, Centre for BioMedical Imaging (CIBM), Lausanne, VD, Switzerland.
Grant sponsor: the Swiss National Science Foundation; Grant number: 320030-143923.
*Correspondence to: Matthias Stuber, Department of Radiology, Vaudois University Hospital Centre (CHUV) / University of Lausanne (UNIL), Lausanne, VD, Switzerland. E-mail: matthias.stuber@chuv.ch
Received 11 July 2013; revised 21 August 2013; accepted 29 August 2013
DOI 10.1002/mrm.24961
Published online 28 October 2013 in Wiley Online Library (wileyonlinelibrary.com).

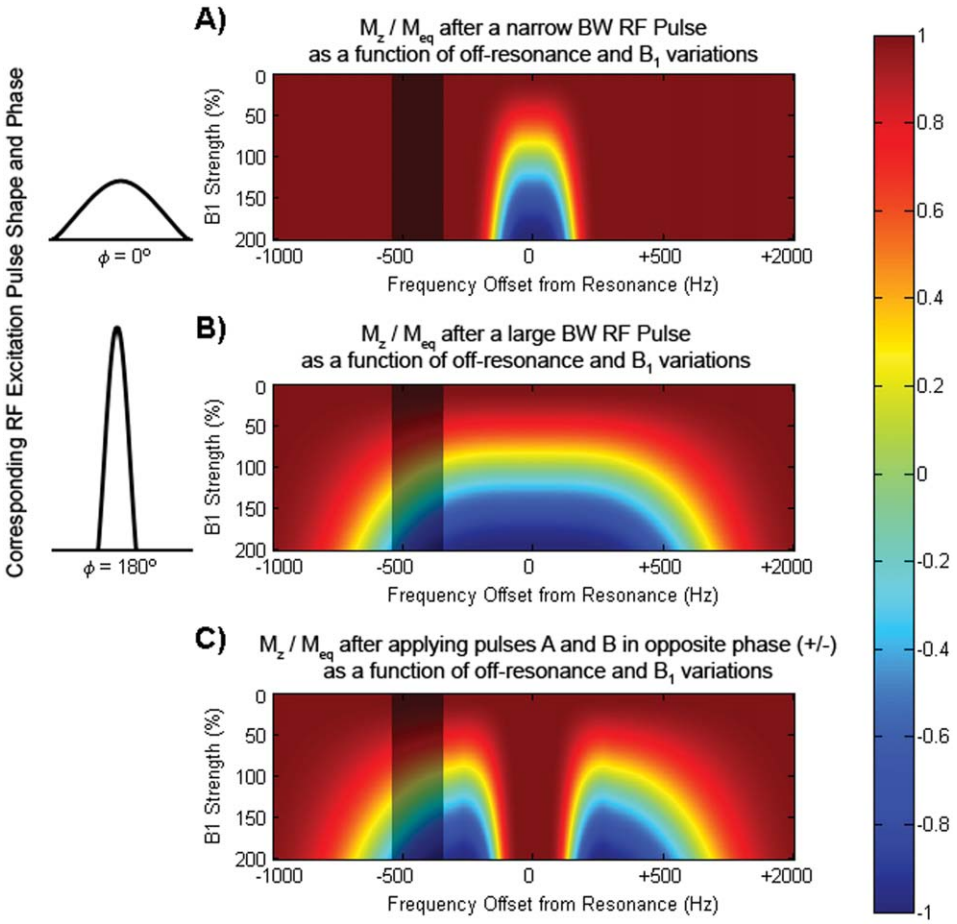

FIG. 1. Conceptual illustration of the water-selective adiabatic T_2-Prep. The color scale represents the longitudinal magnetization, M_z, as a fraction of the available magnetization, M_{eq}. B_1 is given as a percentage, such that a value of 100 corresponds to the desired RF pulse power, with deviations corresponding to B_1 inhomogeneities. (**A**) A narrow bandwidth RF pulse is used to tip M_{Water} into the transverse plane. (**B**) A large-bandwidth RF restoration pulse is used to restore M_{Water}. (**C**) The combination of the two pulses in opposite direction restores M_{Water} (dark red) and tips M_{OffRes} into the transverse plane (green), where it can be spoiled. The shaded region corresponds to the precessional frequencies targeted during fat saturation.

respiratory motion suppression, a T_2-preparation module (7) to enhance contrast between blood and myocardium, a fat saturation prepulse and a spoiled, segmented, k-space gradient echo signal readout. At 3T, a T_2-preparation consisting of two 90° block pulses, with opposite polarity, interspersed by two hyperbolic secant adiabatic 180° pulses (12), has been shown to be most effective. In these implementations, the bandwidth of the RF pulses far exceeds the 440 Hz that separate water and fat frequencies. While this does lead to a T_2-weighted image contrast, no major frequency-dependent change of the water and fat signal is expected after the T_2-Prep. However, by adjusting the bandwidth of selected components of the T_2-Prep, a frequency-selective attenuation of signal may be obtained. Therefore, in our implementation of the frequency selective T_2-Prep, the first radiofrequency (RF) pulse of an adiabatic T_2-Prep was increased in duration, from 0.8 ms to 3.5 ms, reducing its bandwidth from 1250 Hz to 285 Hz, so as to only excite a narrow range of frequencies. As a result, only the magnetization of on-resonance water frequencies (i.e. excluding fat) are tipped into the transverse plane. After the 180° refocusing pulses, a large bandwidth (1250 Hz) RF pulse restores the magnetization of the on-resonance spins (M_{Water}). However, due to its large bandwidth, this final RF pulse of the T_2-Prep also tips the (formerly longitudinal) magnetization of off-resonance spins (M_{OffRes}) into the transverse plane, where their signal is then spoiled. As a result, M_{Water} has been T_2-Prepared, whereas M_{OffRes} (including that of fat) has been spoiled (Fig. 1).

To further reduce fat signal by means of inversion recovery, the RF excitation angles of the first and last pulses (±90°) were increased to ±120°. This approach may then be used alone, or in combination with a typical fat saturation strategy, such as a CHESS pulse (i.e., applied after the T_2-Prep, but before imaging).

Numerical Simulation

The method described above was first characterized numerically. To predict the performance of the WSA-T_2-Prep in the presence of field inhomogeneities, a Bloch equation (13) simulation was implemented using a commercial software package (MATLAB 7.11, The MathWorks Inc., Natick, MA). The excitation and restoration pulses of the WSA-T_2-Prep were modeled as Hamming-windowed sinc functions with durations (800 and 3500 ms) equal to those implemented on the scanner. Taking the Fourier transform of each nonselective RF pulse allows one to then determine its excitation profile as function of precessional frequency. This excitation profile may then be scaled according to B_1 strength, such that the desired RF excitation angle corresponds to a value of 100%. The profiles of the excitation and restoration pulses of the WSA-T_2-Prep may then be predicted

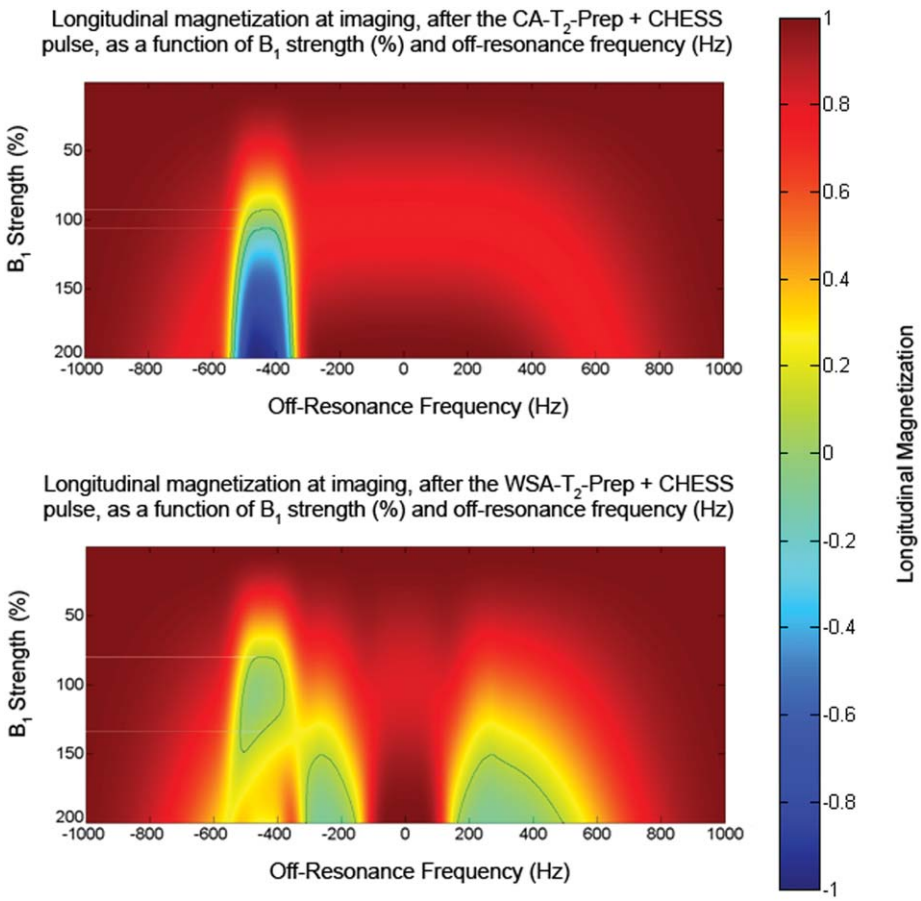

FIG. 2. Comparison of a CHEmically Selective Saturation (CHESS) pulse played out with a conventional adiabatic T_2-Prep (**A**) or in combination with the water-selective adiabatic T_2-Prep (**B**). Scales are as per Figure 1, with the outlined regions corresponding to a signal intensity of between −10% and +10% of M_{eq}. The WSA-T_2+ CHESS combined approach successfully suppresses fat signal across a larger range of B_1 values than does the CHESS pulse of a conventional sequence, demonstrating an improved robustness against RF field inhomogeneities. Specifically, the CHESS pulse reduces fat signal to within ± 10% of its original value for B_1 values of 94–106% of the desired value, whereas the WSA-T_2-Prep+CHESS combination reduces fat signal to within ±10% of its original value for B_1 values of 81–134% of the ideal.

as functions of both B_0 and B_1. These results were plotted, along with a profile of their combined effect, in Figure 1A–C.

The simulation was next expanded to account for the effects of T_1 and T_2 relaxation. Both 180° adiabatic pulses, which rotate magnetization about the z axis, were assumed to perfectly refocus the magnetization. This allowed us to ignore T_2* effects in favor of pure T_2 decay. After each RF excitation pulse, signal evolution was predicted using fat's T_2 (30 ms) and T_1 (200 ms) relaxation times. Other simulation parameters, such as the T_2-Prep time (40 ms), were taken from the sequence parameters described below. 60 ms after the T_2-Prep, a 5 ms long windowed sinc CHESS pulse was applied, which matched the product fat saturation of our scanner. The excitation profile of the CHESS pulse was calculated as described above, with a −440 Hz offset applied. Signal was then allowed to evolve for another 60 ms. Doing so thus allows one to predict the longitudinal magnetization remaining at the time of imaging, as a function of both precessional frequency and B_1 strength. This was done for both the CA-T_2-Prep+CHESS and the WSA-T_2-Prep+CHESS combinations. To illustrate what might be considered "successful" fat suppression, a region was outlined, where the longitudinal magnetization of fat was reduced to between −10% and +10% of its original value (Fig. 2). In each case, this "successful" fat suppression occurs over a certain range of B_1 field strengths. This range was measured to determine which fat suppression technique was most effective at fat's resonance frequency.

Phantom Study

To validate these predictions, a phantom was constructed (14) using agar, $NiCl_2$ (both from Sigma Aldrich, St. Louis, MO), and baby oil (Johnson and Johnson, New Brunswick, NJ), with compartments doped to mimic the relaxation times of blood, myocardium, and fat. This phantom was scanned using both the WSA-T_2-Prep+CHESS pulse sequence and its CA-T_2-Prep+CHESS pulse counterpart. For each combination, the CHESS pulse RF excitation angle was varied from 1° to 360° in steps of 5° (1°, 5°, 10°,...) and plotted versus the fat signal intensity,

as measured in the fat compartment of the phantom. Varying the CHESS pulse RF excitation angle mimics the effect of a B_1 inhomogeneity, as both result in a nonideal fat saturation pulse. Thus, a fat-suppression strategy that works well across a range of excitation angles is also expected to function well in the presence of B_1 inhomogeneities. All images were acquired on a 3T clinical scanner (MAGNETOM Trio, Siemens AG, Healthcare Sector, Erlangen, Germany) using a Cartesian, "artificial ECG"-triggered, 2D segmented k-space spoiled gradient echo sequence, with a field of view (FOV) of 192 × 192 mm^2, a matrix size of 192 × 192, 3.0 mm slice thickness, 15 k-space lines per (simulated) heartbeat, T_2-Prep duration ($TE_{T2\text{-}Prep}$) = 40 ms, RF excitation angle = 15°, echo time (TE) = 2.37 ms, repetition time (TR) = 5.37 ms, and an acquisition time per heartbeat = 80.55 ms. Specific absorption rate (SAR) was recorded from the console of the system.

In Vivo Study

In vivo experiments were performed in nine healthy adult volunteers (ages 24–32 years; four female, five male). Permission from the Institutional Review Board was obtained for all in vivo scans, and written informed consent was obtained from all volunteers before the procedure. For these in vivo scans, the RCA was selected for volume-targeted imaging (15), using an ECG-triggered and navigator-gated three-dimensional (3D) acquisition. The WSA-T_2-Prep and CA-T_2-Prep modules were compared, both with and without an additional CHESS pulse. Imaging parameters for all 4 combinations were as described in the phantom experiments, except for: FOV 360 × 258 mm^2, matrix size 240 × 216 × 20 and a 1.5 mm reconstructed slice thickness (3.0 mm acquired). After acquisition, images were reformatted and analyzed using Soap-Bubble, a semi-automated reformatting and vessel tracking software package (16). Fat suppression efficacy was compared by using vessel sharpness measurements and SNRs, which were measured in selected regions of interest (abdominal fat, epicardial fat, blood, & myocardium). CNRs were also measured between blood and myocardium, to determine the effectiveness of T_2 preparation. A paired 2-tailed Student's t-test was used to analyze the results, with a P-value <0.05 considered statistically significant.

RESULTS

Numerical Simulation

The residual longitudinal magnetization after a narrow bandwidth +90° RF pulse and a large bandwidth −90° RF pulse is illustrated in the Bloch equation simulation shown in Figure 1. This diagram conceptually illustrates the idea behind the WSA-T_2-Prep. After the successive application of an excitation and restoration pulse, M_{Water} is fully restored along the longitudinal axis, whereas all M_{OffRes} are tipped down according to their precessional frequency and the degree of B_1 inhomogeneity they experience (Fig. 1C).

A more comprehensive simulation is presented in Figure 2, which illustrates the residual magnetization after either a solitary CHESS pulse in a conventional T_2-Prepared sequence (A) or a CHESS pulse used in combination with the WSA-T_2-Prep (B). In both graphs, the outlined region corresponds to a residual longitudinal magnetization between −10% and +10%, as described above (see the Methods section).

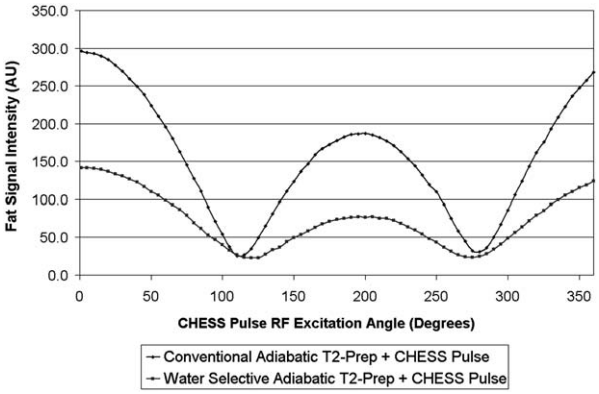

FIG. 3. Signal intensity versus CHESS pulse RF excitation angle measured in the lipid compartment of a multi-compartment phantom, for both the CA-T_2-Prep and the proposed WSA-T_2-Prep. Lower signal intensity indicates greater fat suppression, which should be robust across a range of RF excitation angles. As a B_1 inhomogeneity results in under- or over-tipping of the magnetization, this effect may be modeled by varying the RF excitation angle in a known, homogeneous sample. Note that when using the WSA-T_2-Prep+CHESS combination, not only is fat significantly reduced at non-ideal RF excitation angles, but also that the local minima are significantly broader as compared to the CA-T_2-Prep+CHESS combination. In the extreme case, where there is effectively no CHESS pulse (i.e.: an RF excitation angle of 0° at the y intercept), the WSA-T_2-Prep reduces fat signal by over 50% as compared to the CA-T_2-Prep.

While a CHESS pulse successfully saturates spins at a given frequency, it does so only for a very narrow range of B_1 values. Specifically, at fat's resonance frequency, the CHESS pulse reduces fat signal to within −10 % to +10% of its original value only when the B_1 field strength is within 94–106% of its desired value. This can be seen in Figure 2A, where the degree of saturation drops off rapidly as B_1 variations are introduced. Conversely, when a CHESS pulse is combined with the WSA-T_2-Prep, it remains effective over a large range of B_1 values, as seen in Figure 2B. Specifically, this combined approach reduces fat signal to within −10% to +10% of its original value when the B_1 field strength is within 81–134% of its desired value. Thus, according to the numerical simulations, the WSA-T_2-Prep+CHESS pulse approach should be far more robust against B_1 inhomogeneities than a CHESS pulse acting in combination with a CA-T_2-Prep. Note that the WSA-T_2-Prep+CHESS pulse's effectiveness is also maintained over a relatively broad range of frequencies than for WSA-T_2-Prep+CHESS approach.

Phantom Study

Experimental validation of these simulations is demonstrated in Figure 3, which shows the results of the

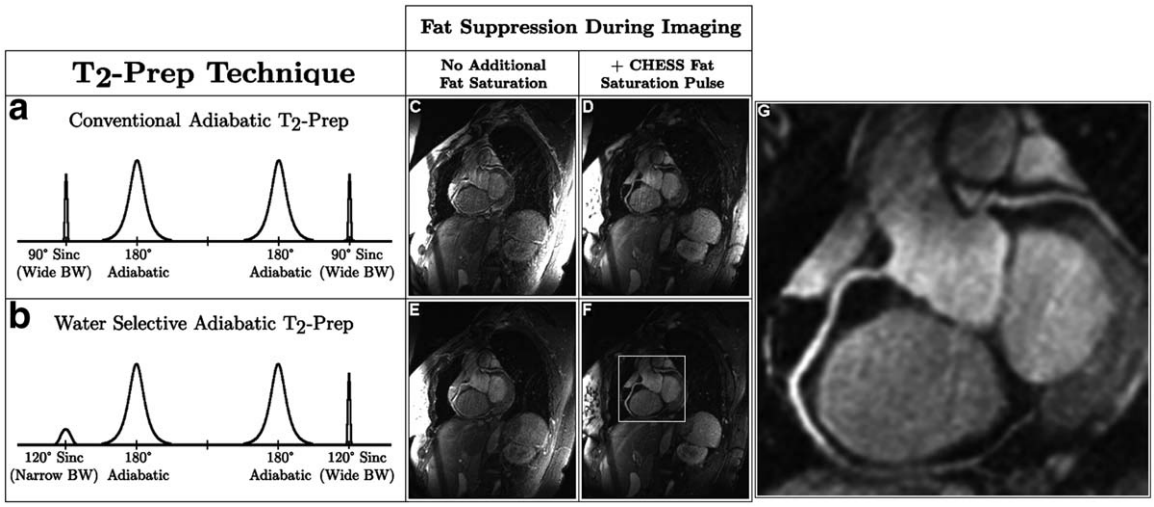

FIG. 4. Representative in vivo images of the right coronary artery, using different fat saturation approaches. Images in the top row (**C,D**) were acquired using a conventional adiabatic T_2-Prep (**A**), whereas images in the bottom row (**E,F**) were acquired using the water-selective adiabatic T_2-Prep (**B**). Likewise, images in the right column (D,F) were acquired using a CHESS pulse, whereas images in the left column (C,E) were acquired without any additional fat saturation. While the CHESS pulse suppresses epicardial fat well, it does so poorly for abdominal fat, possibly due to B_1 inhomogeneities. As a result, this allows the abdominal fat to cause visible respiratory ghosting artifacts in the image. However, in both the CHESS and non-CHESS sequences, the WSA-T_2-Prep improved fat suppression in both epicardial and abdominal fat as compared to the CA-T_2-Prep. Vessel sharpness also improved due to decreased epicardial fat signal and reduced background noise (as seen in G).

phantom study. The signal intensity of fat (arbitrary units) is plotted versus the RF excitation angle used for the CHESS pulse. Deviations from the optimal RF excitation angle (i.e., the one that maximally suppresses fat signal) may once again be considered as equivalent to a B_1 inhomogeneity. As can be seen, the WSA-T_2-Prep+CHESS combination suppresses fat signal more effectively at nonideal B_1 values than does the CA-T_2-Prep+CHESS combination. Not only is the overall signal intensity of fat reduced, but more importantly, the local minima are significantly broader when using the WSA-T_2-Prep+CHESS combination as compared to CA-T_2-Prep+CHESS. In the extreme case, where there is no effective CHESS pulse (i.e., at a CHESS pulse RF excitation angle that approaches 0°, at the y-intercept), the WSA-T_2-Prep reduces fat signal by over 50% as compared to the CA-T_2-Prep. Any differences in SAR fell below 1%, the detection threshold of the MRI console.

In Vivo Study

Sample images from the volunteer study are shown in Figure 4, with corresponding SNR and CNR measurements in Table 1. When the WSA-T_2-Prep was used as the sole fat saturation strategy (i.e., with no CHESS pulse), abdominal and epicardial fat SNRs were reduced by 38% ($P < 0.002$) and 20% ($P < 0.01$), respectively, as compared to using the CA-T_2-Prep. This was due to both a reduction in the absolute signal intensities of the fat signal, as well as a decrease in background noise (see Table 1). As a consequence, the WSA-T_2-Prep increased the blood SNR from 59.8 to 71.9 ($P = 0.07$) and the myocardium SNR from 36.9 to 42.3 ($P = 0.28$) versus the CA-T_2-Prep, though neither of these were statistically significant. However. the change in CNR between blood and myocardium was significant, increasing from 22.9 to 29.6 ($P < 0.05$). Additionally, vessel sharpness increased from 46.1% to 49.4% ($P < 0.05$) when the WSA-T_2-Prep was

Table 1
Image Properties for Select Fat Saturation Strategies

	T_2-Prep without a CHESS pulse		T_2-Prep + CHESS Fat Saturation Pulse	
	Conventional Adiabatic T_2-Prep	Water-Selective Adiabatic T_2-Prep	Conventional Adiabatic T_2-Prep	Water-Selective Adiabatic T_2-Prep
Abdominal Fat SNR $\pm\sigma$	312.6 ± 116.2	192.3 ± 73.0[a]	162.3 ± 72.8	63.8 ± 30.8[a]
Epicardial Fat SNR $\pm\sigma$	103.9 ± 49.6	83.1 ± 50.9[a]	28.0 ± 9.1	17.8 ± 4.6[a]
Blood SNR $\pm\sigma$	59.8 ± 16.2	71.9 ± 14.4	69.8 ± 18.5	73.2 ± 19.9
Myocardium SNR $\pm\sigma$	36.9 ± 12.7	42.3 ± 20.5	35.3 ± 10.1	42.9 ± 11.9
Blood-Myocardium CNR $\pm\sigma$	22.9 ± 9.6	29.6 ± 10.7[a]	34.5 ± 12.6	30.4 ± 9.5
RCA Vessel Sharpness $\pm\sigma$	46.1% ± 8.0%	49.4% ± 8.3%[a]	66.5% ± 6.1%	72.2% ± 5.5%[a]
Background Noise (AU) $\pm\sigma$	1.8 ± 0.6	1.4 ± 0.3[a]	1.5 ± 0.2	1.3 ± 0.1[a]

[a]Indicates a statistically significant difference between the Conventional Adiabatic T_2-Prep T_2-Prep and the Water-Selective T_2-Prep ($P<0.05$).

used in place of the CA-T_2-Prep. In one volunteer, epicardial fat signal made vessel tracking impossible in the CA-T_2-Prep case and the related vessel sharpness measurements were excluded from the results.

When combined with a CHESS pulse, the WSA-T_2-Prep continued to improve fat suppression as compared to the CA-T_2-Prep+CHESS combination. Abdominal and epicardial fat SNR were reduced by 61% and 37% (both $P < 0.005$), respectively. Blood SNR increased nonsignificantly, from 69.8 to 73.2 ($P = 0.31$), as did myocardium SNR, from 35.3 to 42.9 ($P = 0.09$). As a result of this increased myocardium signal, the WSA-T_2-Prep+CHESS combination slightly reduced the CNR between blood and myocardium, as compared to the CA-T_2-Prep+CHESS combination, from 34.5 to 30.4, though this was not statistically significant ($P = 0.21$). However, the WSA-T_2-Prep+CHESS combination did significantly increase vessel sharpness from 66.5% to 72.2% ($P < 0.05$) as compared to the CA-T_2-Prep+CHESS combination. Overall, the combined WSA-T_2-Prep+CHESS fat saturation strategy had the greatest reduction in abdominal and epicardial fat signals, as well as the highest vessel sharpness in the coronary arteries.

DISCUSSION

The WSA-T_2-Prep, in combination with a CHESS pulse, leads to a more B_0- and B_1-independent fat saturation than does a CHESS pulse in a conventional sequence. This modification adds no time constraints to the sequence and has a negligible effect on SAR.

The reasons for this improved performance are likely due to the nature of the WSA-T_2-Prep. A CHESS pulse suppresses signal by applying a certain amount of power at a certain frequency, leaving the method susceptible to inhomogeneities in either the power delivered or the expected frequency of excitation. With lower field strengths or perfect shimming, this may be sufficient. However, at higher field strengths or in regions of magnetic field susceptibility, CHESS pulses may rapidly lose their effectiveness. This mechanism of action differs from that of the WSA-T_2-Prep, however, which suppresses signal on an exclusionary basis. Off-resonance spins, regardless of their exact precessional frequency, are eliminated. As such, it is inherently robust against B_0 variations.

After the WSA-T_2-Prep, off-resonance spins, such as fat, do begin to recover, but they do so only partially. As a result, the subsequent CHESS pulse acts on a lower initial fat magnetization than if it were applied on its own. This limits the problem of imperfect saturation caused by B_1 inhomogeneities.

Some potential limitations of the technique do exist. One is a possible loss of T_2 contrast between the blood and myocardium. Specifically, as the RF excitation angles of first and last pulse of the WSA-T_2-Prep have been increased from $\pm 90^\circ$ to $\pm 120^\circ$, only 87% of the magnetization is T_2-Prepared ($\sin(120^\circ) = 0.87$). Thus, one might expect a slight decrease in CNR. However, a benefit of reducing the overall fat signal is that respiratory ghosting artifacts originating from areas with high fat signal intensities are minimized. Such a reduction in artifactual background signal may then contribute to a lower measured "noise", which is consistent with previous findings (17,18). Thus, despite the over-tipped magnetization, the net effect on blood/myocardium CNR is not significant (see the Results section). In fact, the blood/myocardium CNR slightly improves in the "no CHESS pulse" case.

The use of $\pm 120^\circ$ pulses also introduces the possibility that short T_1 species, such as the liver, may recover sufficiently during T_2-Prep such that their longitudinal magnetization approaches zero during the subsequent navigator echoes. This was occasionally seen during protocol development, particularly in the case of long T_2-Prep durations, but was not encountered with the T_2-Prep durations used in the experiments described above.

A further limitation of this study was that only the RCA was selected for imaging. The RCA is embedded in fat over a long stretch of tissue and may, therefore, be particularly well suited for analysis when testing a new fat saturation technique. However, as other vessels were not examined, the performance of the WSA-T_2-Prep in other anatomical regions may need to be evaluated.

Practically speaking, and as with any sequence, it may also be necessary to adjust the CHESS pulse RF excitation angle, depending on the precise combination of prepulses, k-space acquisition order, and other imaging parameters.

In terms of novelty, this work is not the first to propose modifying a T_2-Prep sequence for improved fat saturation. A previous approach, described by Nezafat et al (4), used a T_2-Prep composed of a reverse adiabatic half-passage pulse, followed by an adiabatic fast passage pulse, followed by a final (nonreversed) adiabatic half-passage pulse. A small additional delay, δ, is introduced between last two pulses, resulting in a residual 90° phase difference between water and fat isochromats. As a result, water is restored by the final adiabatic pulse, whereas fat is not. This fat magnetization, which remains transverse, is then spoiled. One shortcoming of this innovative approach may be its sensitivity to field inhomogeneities, as phase dispersion may result in a nonideal phase difference between water and fat spins. Additionally, in the reported implementation, the (reverse) adiabatic half passage pulse tips fat magnetization into the transverse plane and thus may not introduce the degree of inversion recovery found in the WSA-T_2-Prep approach. However, a side-by-side comparison of these techniques may still be useful.

Another obvious choice for improved fat saturation in coronary MRA includes the use of Dixon methods (17). In cases where cardiac fat has a diagnostic value, such an approach may be interesting. However, as Dixon methods necessarily require, at minimum, the acquisition of an additional echo, an increase in scan time or a decrease in temporal resolution may have to be considered.

An alternative to fat saturation is the use of spectrally selective excitation pulses (19). Börnert et al (20) have demonstrated that these approaches have similar effectiveness to spectral presaturation. While interesting, spectral pulses may take significantly longer than their nonfrequency selective counterparts, mandating longer

minimum echo and repetition times, which may, in turn, increase sensitivity to motion or adversely affect scanning time in coronary MRA. That being said, the use of spectral spatial pulses is completely compatible with the WSA-T_2-Prep method proposed above, as the type of RF pulses used for imaging has no influence on the magnetization preparation modules.

In summary, the WSA-T_2-Prep, while maintaining T_2 enhancement characteristics of the T_2-Prep, significantly augments the abdominal and epicardial fat saturation when combined with a conventional CHESS pulse. The WSA-T_2-Prep also leads to significant fat signal suppression when no other fat saturation strategy is used. These in vivo results were consistent with numerical simulations and phantom work, and as a result of this improved fat suppression, the vessel sharpness of the RCA was significantly improved, resulting in a greater conspicuity of the vessel.

ACKNOWLEDGMENTS

Additional support was provided in part by the Centre d'Imagerie BioMedical (CIBM) of the UNIL, EPFL, UNIGE, CHUV, and HUG, as well as the Jeantet and Leenaards Foundations.

REFERENCES

1. Bydder GM, Young IR. MR imaging: clinical use of the inversion recovery sequence. J Comput Assist Tomogr 1985;9:659–675.
2. Bottomley PA, Foster TH, Leue WM. In vivo nuclear magnetic resonance chemical shift imaging by selective irradiation. Proc Natl Acad Sci U S A 1984;81:6856–6860.
3. Haase A, Frahm J, Hanicke W, Matthaei D. 1H NMR chemical shift selective (CHESS) imaging. Phys Med Biol 1985;30:341–344.
4. Nezafat R, Ouwerkerk R, Derbyshire AJ, Stuber M, McVeigh ER. Spectrally selective B1-insensitive T2 magnetization preparation sequence. Magn Reson Med 2009;61:1326–1335.
5. Dixon WT. Simple proton spectroscopic imaging. Radiology 1984; 153:189–194.
6. Wen H, Denison TJ, Singerman RW, Balaban RS. The intrinsic signal-to-noise ratio in human cardiac imaging at 1.5, 3, and 4 T. J Magn Reson 1997;125:65–71.
7. Brittain JH, Hu BS, Wright GA, Meyer CH, Macovski A, Nishimura DG. Coronary angiography with magnetization-prepared T2 contrast. Magn Reson Med 1995;33:689–696.
8. Wright GA, Nishimura DG, Macovski A. Flow-independent magnetic resonance projection angiography. Magn Reson Med 1991;17: 126–140.
9. Botnar RM, Stuber M, Danias PG, Kissinger KV, Manning WJ. Improved coronary artery definition with T_2-weighted, free-breathing, three-dimensional coronary MRA. Circulation 1999;99:3139–3148.
10. van Heeswijk RB, Feliciano H, Bongard C, et al. Free-breathing 3 T magnetic resonance T_2-mapping of the heart. JACC Cardiovasc Imaging 2012;5:1231–1239.
11. Nezafat R, Stuber M, Ouwerkerk R, Gharib AM, Desai MY, Pettigrew RI. B1-insensitive T2 preparation for improved coronary magnetic resonance angiography at 3 T. Magn Reson Med 2006;55:858–864.
12. Hwang TL, van Zijl PC, Garwood M. Fast broadband inversion by adiabatic pulses. J Magn Reson 1998;133:200–203.
13. Bloch F, Hansen W, Packard M. Nuclear induction. Phys Rev 1946; 70:460–474.
14. Kraft KA, Fatouros PP, Clarke GD, Kishore PRS. An MRI phantom material for quantitative relaxometry. Magn Reson Med 1987;5:555–562.
15. Stuber M, Botnar RM, Danias PG, et al. Double-oblique free-breathing high resolution three-dimensional coronary magnetic resonance angiography. J Am Coll Cardiol 1999;34:524–531.
16. Etienne A, Botnar RM, Van Muiswinkel AM, Boesiger P, Manning WJ, Stuber M. "Soap-Bubble" visualization and quantitative analysis of 3D coronary magnetic resonance angiograms. Magn Reson Med 2002;48:658–666.
17. Börnert P, Koken P, Nehrke K, Eggers H, Ostendorf P. Water fat resolved whole-heart Dixon coronary MRA: an initial comparison. In Proceedings of the 20th Annual Meeting of ISMRM, Melbourne, Australia, 2012. p. 316.
18. Lu D, Saini S, Hahn P, Goldberg M, Lee M, Weissleder R, et al. T_2-weighted MR imaging of the upper part of the abdomen: should fat suppression be used routinely? AJR Am J Roentgenol 1994;162: 1095–1100.
19. Meyer CH, Pauly JM, Macovski A, Nishimura DG. Simultaneous spatial and spectral selective excitation. Magn Reson Med 1990;15: 287–304.
20. Börnert P, Stuber M, Botnar RM, Kissinger KV, Manning WJ. Comparison of fat suppression strategies in 3D spiral coronary magnetic resonance angiography. J Magn Reson Imaging 2002;15:462–466.